SCIENTIFIC REPORTS

OPEN

SUBJECT AREAS:
SURFACES, INTERFACES AND THIN FILMS
MAGNETIC PROPERTIES AND MATERIALS
FERROELECTRICS AND MULTIFERROICS

Received
31 July 2013

Accepted
13 November 2013

Published
2 December 2013

Correspondence and requests for materials should be addressed to C.L.L. (cllu@mail.hust.edu.cn) or J.M.L. (liujm@nju.edu.cn)

Polarization enhancement and ferroelectric switching enabled by interacting magnetic structures in $DyMnO_3$ thin films

Chengliang Lu[1], Shuai Dong[2], Zhengcai Xia[1], Hui Luo[1], Zhibo Yan[3], Haowen Wang[1], Zhaoming Tian[1], Songliu Yuan[1], Tao Wu[4] & Junming Liu[3,5]

[1]School of Physics & Wuhan National High Magnetic Field Center, Huazhong University of Science and Technology, Wuhan 430074, China, [2]Department of Physics, Southeast University, Nanjing 211189, China, [3]Laboratory of Solid State Microstructures, Nanjing University, Nanjing 210093, China, [4]Physical Sciences and Engineering Division, King Abdullah University of Science and Technology, Thuwal, 23955-6900, Saudi Arabid, [5]Institute for Advanced Materials, South China Normal University, Guangzhou 510006, China.

The mutual controls of ferroelectricity and magnetism are stepping towards practical applications proposed for quite a few promising devices in which multiferroic thin films are involved. Although ferroelectricity stemming from specific spiral spin ordering has been reported in highly distorted bulk perovskite manganites, the existence of magnetically induced ferroelectricity in the corresponding thin films remains an unresolved issue, which unfortunately halts this step. In this work, we report magnetically induced electric polarization and its remarkable response to magnetic field (an enhancement of ~800% upon a field of 2 Tesla at 2 K) in $DyMnO_3$ thin films grown on Nb-$SrTiO_3$ substrates. Accompanying with the large polarization enhancement, the ferroelectric coercivity corresponding to the magnetic chirality switching field is significantly increased. A picture based on coupled multicomponent magnetic structures is proposed to understand these features. Moreover, different magnetic anisotropy related to strain-suppressed $GdFeO_3$-type distortion and Jahn-Teller effect is identified in the films.

Multiferroics with coexisting and intimately coupled ferroelectric (FE) and magnetic orders, have attracted considerable attentions due to their vast application potentials and fundamental interest in the past decade[1–6]. It has been confirmed that a series of magnetic configurations can break the spatial inversion symmetry and thus produce spontaneous polarization (P)[4]. One of the most frequently cited evidences is the spiral-spin-ordering (SSO) in orthorhombic manganites $R\mathrm{MnO_3}$ (R = Tb and Dy), as highlighted by the first discovery of multiferroicity and giant magnetoelectric (ME) coupling in bulk $\mathrm{TbMnO_3}$ (TMO) in 2003[7]. For these model multiferroics with SSO, successive phase transitions occur due to the proximate free energies of various phases in the low temperature (T) region. Upon cooling, the multiferroic $R\mathrm{MnO_3}$ enters a collinear sinusoidal antiferromagnetic (AFM) state at T_N (~40 K) from a paramagnetic (PM) one, and then the SSO develops with a locked period at T_C (~20–30 K) and an improper FE polarization arises simultaneously via the inverse Dzyaloshinskii-Moriya (DM) interaction between adjacent spins. The as-generated P can be expressed as $\boldsymbol{P} \propto \boldsymbol{e}_{ij} \times (\boldsymbol{S}_i \times \boldsymbol{S}_j)$, where $\boldsymbol{e}_{ij}$ denotes the unit vector connecting the two spins $\boldsymbol{S}_i$ and $\boldsymbol{S}_j$. Upon further decreasing temperature to $T < 10$ K, the moment of rare-earth ions forms a long range ordering at T_R and also modulates the ferroelectricity[4,8].

To date, bulk SSO multiferroic manganites including single crystals have been intensively studied, and the associated physics has been progressively understood[9–12]. However, research on the thin films is rare, and the insights are expected to play a core role in designing advanced multifunctional devices. From the fundamental viewpoint, fabrication of thin films will introduce additional degrees of freedom such as strain to mediate the multiferroicity besides the bulk-related routes, e.g., chemical doping. It is thus reasonable to expect intriguing properties in thin films since the delicate balance among different exchange interactions is sensitive to internal/external perturbations in multiferroic manganites. Indeed, a few recent papers reported emergent ferromagnetism related to the modified lattice distortion in TMO thin films, while no ferroelectricity associated with the SSO

was captured[13–18]. This is quite different from the E-type AFM multiferroic manganite thin films, in which the magnetic ferroelectricity was reported in several materials[19–21].

According to the phase diagram of perovskite manganites, the SSO phase is rather sensitive to structure distortion, and can only exist within a very narrow region[22]. Furthermore, the SSO in $BiFeO_3$ was revealed to be suppressed by strain[23,24]. It thus seems reasonable to expect the suppression of SSO phase by strain in orthomanganite thin films. However, while the ground state of bulk $YMnO_3$ is the E-type AFM[20,21,25], a strain-induced SSO phase accompanied by spontaneous polarization was reported in the corresponding thin films recently[26]. In a recent ultrafast optical spectroscopy study, an anomaly around $T = 30$ K (close to the FE Curie temperature $T_C \sim 28$ K of TMO single crystal) was observed in TMO thin films, which hints the coexistence of SSO and ferroelectricity but no relevant data were reported[27]. These works motivated us to explore the SSO induced ferroelectricity and the ME coupling in orthorhombic $RMnO_3$ thin films.

Along this line, we choose $DyMnO_3$ (DMO) thin films as the prototype to investigate the possible coexistence of multiple ferroic-orders and the ME coupling among them. Besides TMO, DMO is one of the typical multiferroic manganites with SSO, and they possess quite similar physical properties. Particularly, in both materials, the SSO induces ferroelectricity through the inverse DM interaction, and magnetic field switches polarization from the c axis to the a axis (P flopping)[8]. DMO lies far inside the SSO region in the magnetic phase diagram while TMO is somehow in the vicinity of the A-type AFM region, allowing more flexibility for spin order modulation in DMO than TMO[22]. In addition, DMO single crystal exhibits much larger spontaneous polarization ($P \sim 2100$ μC/m^2) than that of TMO ($P \sim 600$ μC/m^2)[8], which facilitates reliable measurements. More importantly, in bulk DMO, the Dy moments play a much more active role through the Dy-Mn interaction in generating FE polarization than the Tb moments in TMO, enabling fascinating physics unavailable in TMO[28–33].

In this work, we perform systematic experiments to investigate the structural, magnetic, dielectric, and ferroelectric properties of strained DMO thin films grown on Nd-$SrTiO_3$ (001) (NSTO). Magnetically induced ferroelectricity was clearly identified using the pyroelectric current method and the direct electric hysteresis loop measurement. Interestingly, both the polarization and ferroelectric coercivity can be significantly enhanced by magnetic field at $T < T_R$, indicating the essential role of Dy moment on ferroelectricity. In addition, different magnetic anisotropy was observed. Notably, these multiferroic behaviors in DMO thin films are quantitatively different from but qualitatively similar to those for bulk DMO crystals, indicating that the strain may play a non-negligible role in modulating multiferroicity in such manganite thin films.

Results

Fig. 1(a) presents the high resolution X-ray diffraction (HRXRD) pattern of one typical DMO/NSTO thin film, in which pure c-axis orientation can be seen for the film. The out-of-plane (OOP) lattice parameter of the film was found to be ~7.393 Å, which is larger than that of the bulk counterpart, indicating an in-plane compressive strain. Fig. 1(b) shows the rocking curve around the (002) reflection for the film, and the full width half maximum (FWHM) is ~0.72°. The NSTO substrate has a cubic crystalline structure with lattice parameter $a = 3.905$ Å, while the orthorhombic DMO has lattice parameters $a = 5.278$ Å, $b = 5.834$ Å, and $c = 7.378$ Å[34]. Therefore, large lattice misfit is expected in the epitaxial growth. To get detailed information of the epitaxial growth, we perform asymmetric reciprocal space mapping (RSM) of the $(103)_C$ and $(113)_C$ reflections where the subscript 'C' refers to the pseudo-cubic lattice, and the data are shown in Fig. 1(c) and (d), respectively. Identical in-plane (IP) lattice parameters of the film with respect to the substrate can be

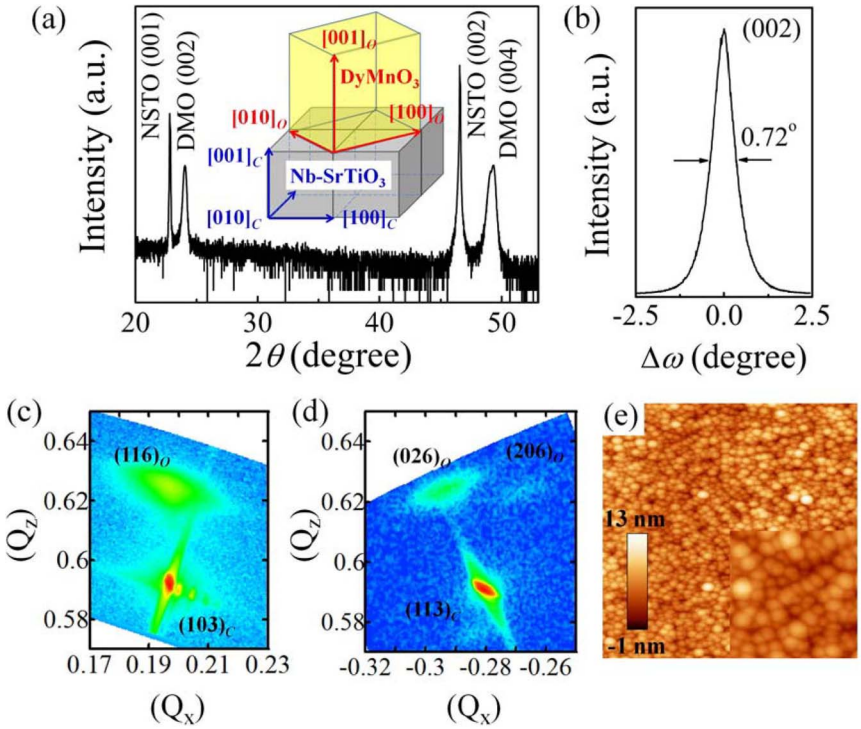

Figure 1 | (a) Symmetric X-ray θ-2θ scan of the DMO/NSTO thin film. The inset shows a schematic drawing of the epitaxial growth of DMO on (001) NSTO. (b) Rocking curve around the (002) reflection for the film. The FWHM is ~0.72°. (c) and (d) present the data of reciprocal space mapping around the $(103)_C$ and $(113)_C$ reflections of the substrates, respectively. (e) 2 × 2 μm^2 atomic force microscopy image of the film, in which islands dominate the surface morphology. The R_{rms} of film is estimated to be ~1.6 nm. The inset shows the topography with a smaller scanning size of 0.5 × 0.5 μm^2, in which the island size can be derived to range from 40 nm to 80 nm.

seen from the $(103)_C$ reflection, indicating the coherent growth of the film on the substrate. However, two diffraction spots corresponding to $(206)_O$ and $(026)_O$ can be observed in Fig. 1(d), which suggests an orthorhombic twin crystalline structure of the film and thus consisting with the relative large FWHM of (002) reflection. The subscript 'O' refers to the orthorhombic lattice. Based on the RSM data, a sketch of the stacking model of DMO unit cells on NSTO substrate is shown in the inset of Fig. 1(a). A similar growth model was previously proposed for TMO thin films[35]. Moreover, the atomic force microscopy image (Fig. 1 (e)) shows an island surface for the film. The root-mean-square roughness (R_{rms}) of the film is estimated to be 1.6 nm, and the island size ranges from 40 nm to 80 nm. In addition, lattice parameters (and the corresponding variation ratio) of the orthorhombic DMO thin films can be estimated from the RSM data as, $a = 5.288$ Å (0.2%), $b = 5.770$ Å (−1.1%), and $c = 7.395$ Å (0.2%). Considering the relatively large uniaxial compressive strain along the b axis, we expect certain anisotropy in the physical properties of the film.

The T-dependences of magnetization (M) in the ab plane and along the c axis are measured under both field cooling (FC) and zero field cooling (ZFC) conditions, and the data are shown in Fig. 2(a). For both cases, the magnetization evolves smoothly with T until $T_R \sim 9$ K, at which distinct anomalies in the $M(T)$ curves are observed and can be associated with the long range ordering of Dy moment. Usually, the large paramagnetic contribution of Dy moment will dominate the magnetic signal, and make the detection of AFM (or SSO) phase transition difficult, as reported for bulk DMO single crystal[36]. Although identical T_R is evidenced from the data in the ab plane and along the c axis, the clear difference in shapes of the $M(T)$ curves implies the possible magnetic anisotropy within the films. In Fig. 2 (b) and (c), the $M(H)$ curves measured under various temperatures are plotted. We calculate the demagnetization factor to be $\sim 10^{-4}$ in the ab plane and ~ 1 along the c axis for our sample (area: 3 mm × 3 mm, thickness: 300 nm), which gives rise to the demagnetization field of ~1 Oe in the ab plane and ~560 Oe along the c axis at $H = 7$ T[37]. Therefore, the demagnetization field only has very weak contribution to our magnetic measurements. Evidently, the magnetization of ab plane is much larger than that of c axis, which confirms the magnetic anisotropy in the films. A close examination of the $M(H)$ curves reveals that the maximum magnetization ($H = 7$ T and $T < T_R$) are $M_m{}^{ab} \sim 10.3$ $\mu_B/f.u.$ for ab plane and $M_m{}^{c} \sim 1.08$ $\mu_B/f.u.$ for c axis, which gives the magnetic anisotropy as large as $M_m{}^{ab}/M_m{}^{c} \sim 10$. For DMO bulk single crystal, the magnetization at $H = 7$ T and $T < T_R$ was reported to be ~7.5 $\mu_B/f.u.$ for b aixs, ~4.1 $\mu_B/f.u.$ for a aixs[31], and ~2.5 $\mu_B/f.u.$ for c axis which is obtained by an extrapolation considering the linear $M(H)$ curve[38], giving rise to the magnetic anisotropy to be $M_m{}^{a}/M_m{}^{c} \sim 1.7$ and $M_m{}^{b}/M_m{}^{c} \sim 3$. In Ref. 36, the $M_m{}^{b}$ of bulk DMO was reported to be ~8.6 $\mu_B/f.u.$, leading to a slightly larger magnetic anisotropy $M_m{}^{b}/M_m{}^{c} \sim 3.4$. Clearly, the magnetic anisotropy of bulk DMO is smaller than that of the thin films. Interestingly, a clear metamagnetic transition occurs around $H = 1.5$ T below T_R, marked by an arrow in Fig. 2(b), which was typically observed in bulk SSO multiferroic manganites and associated with the rare-earth moments[8]. It is worthy of noting that such metamagnetic phase transition is always accompanied by large variation in P due to the one-to-one correspondence between ferroelectric and magnetic orders[8]. Therefore, we explore the possible ferroelectricity and ME coupling in our DMO thin films by carrying out detailed dielectric and ferroelectric measurements as a function of temperature and magnetic field.

From the T-dependent data of dielectric susceptibility ε_c and polarization P_c shown in Fig. 3, multiple phase transitions can be identified. In Fig. 3(a), a small change in ε_c arises at $T_N = 40$ K due to the ordering of Mn moments. Importantly, a pronounced peak at $T_C = 21$ K can be observed in $\varepsilon_c(T)$, and a corresponding emergence of P_c is identified in the $P_c(T)$ plot in Fig. 3(b). According to the phase

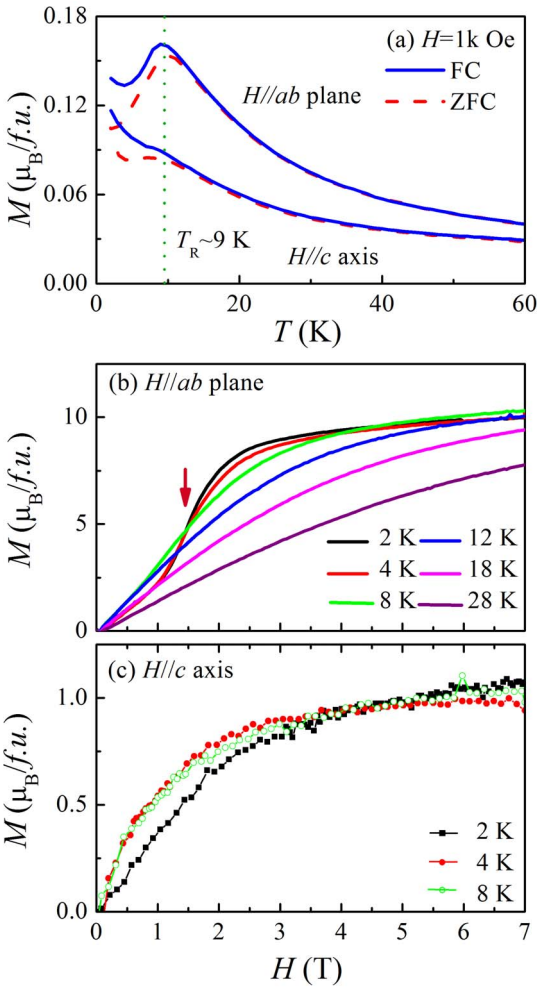

Figure 2 | (a) Temperature dependence of magnetization measured in the ab plane and along the c axis. Measured H dependence of magnetization in the ab plane (b) and along the c axis (c) at various temperatures. The arrow in (b) marks the metamagnetic transition.

diagram of orthorhombic perovskite manganites, two magnetic configurations, i.e. the SSO and E-type AFM orders, can break the spatial inversion symmetry and thus produce a spontaneous polarization[22], while the latter has a spontaneous polarization along the a-axis[39,40]. Moreover, a recent first-principles calculation predicted that the E-AFM multiferroic phase can only be induced by large tensile strain (5%)[41]. Therefore, the polarization P_c of the compressively strained thin films should origin from the SSO via the DM interaction, similar to the bulk counterpart[9–11]. The SSO induced ferroelectric state is further attested by the well-shaped polarization-electric field (P-E) hysteresis loop, as shown in Fig. 3(c). Generally, in SSO multiferroics, the reversal of polarization from $+P_c$ to $-P_c$ corresponds to the reversal of spin chirality ($\boldsymbol{Q} = \boldsymbol{S}_i \times \boldsymbol{S}_j$) from clockwise $\boldsymbol{Q}_{-a}$ ($bc-$) to counterclockwise $\boldsymbol{Q}_a$ ($bc+$) (or vice versa), marking the close link between magnetic and ferroelectric orders[42].

Further cooling the film down to $T \sim 12$ K, both $\varepsilon_c(T)$ and $P_c(T)$ (red circles in Fig. 3(b)) abruptly decrease, indicating a possible transition between different magnetic configurations. Actually, similar features were also observed in bulk DMO, and a SSO to commensurate (CM) AFM phase transition of Dy moment was considered as the origin[30–33]. In details, Dy moments form a SSO phase with the same propagation vector as the Mn magnetic lattice ($\tau^{Dy} = \tau^{Mn} = 0.385b$) at 15 K ($< T_C \sim 18$ K), due to the Dy-Mn spin interaction, and then make an additional contribution to P_c[30]. Further cooling causes a suppression of the Mn-promoted SSO of the Dy moment,

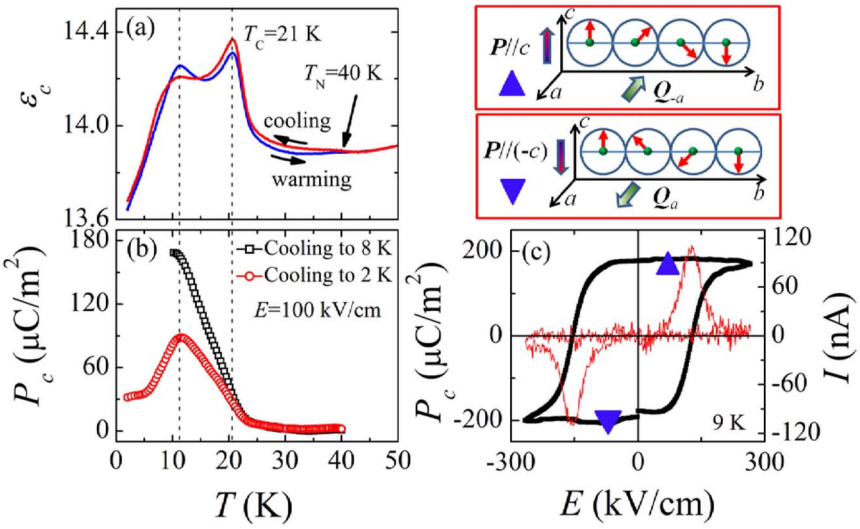

Figure 3 | Temperature dependence of ε_c (a) and P_c (b). The arrows in (a) indicate the directions of the heating or cooling processes. Red circles and black squares in (b) correspond to the results of different poling processes. In (c), ferroelectric hysteresis loop measured at $T = 9$ K without magnetic field during the cooling process. In the upper of (c), a sketch of the clockwise (Q_{-a}) and counterclockwise (Q_a) spiral spin orders is presented, corresponding to the $+P_c$ and $-P_c$, respectively.

and a CM/AFM configuration with $\tau^{Dy} = 0.5$b arises because of the dominance of the Dy-Dy interaction over the Dy-Mn spin coupling at $T < T_R$[31–33]. As a consequence, abrupt decrease in P_c and ε_c occurs, as observed in the $P_c(T)$ and $\varepsilon_c(T)$ data of the film (Fig. 3(a) and (b)). Moreover, microscopic evidences revealed significant thermal hysteresis for the first order SSO-CM/AFM phase transition of Dy[33], which suggests a strong thermal history dependence of the microscopic process related to the emergence of FE polarization. To confirm this point, we poled the films using the same electric field down to 8 K (close to T_R), and then the polarization was collected by integrating the pyroelectric current. Remarkably different P_c data evolving with T for the two measuring processes were indeed obtained as shown in Fig. 3(b), indicating the important role of Dy moment to the improper ferroelectricity in the films.

To further explore the coupling between magnetic and ferroelectric orders, which in turn would be helpful for us to comprehensively understand the physics of multiferroicity in DMO thin films, we measure the T-dependent ε_c and P_c under various magnetic fields. As displayed in Fig. 4, rather different magnetic responses of $\varepsilon_c(T)$ and $P_c(T)$ can be identified when H is applied along the c-axis or in the ab plane. For $H//c$ axis, no substantial H dependence in P_c is seen although T_C is slightly suppressed with increasing H. For $H//ab$ plane, remarkable enhancement in P_c is observed, and a maximum value of $P_c(2T)/P_c(0T) \sim 9$ is estimated at $T = 2$ K. Correspondingly, the abrupt decrease in ε_c below 12 K, induced by the long range ordering of Dy moment, is significantly suppressed by $H//ab$ plane, indicating the essential role of Dy moment in mediating the FE polarization in the films. At $H > 5$ T, the FE phase transition in $\varepsilon_c(T)$ becomes dispersive, and as a consequence P_c is largely suppressed even in the temperature region $T > T_R$. It implies possible P-flopping due to the rotation of the bc-spiral to the ab-spiral caused by $H//ab$ plane.

In Fig. 5, the H dependence of pyroelectric current I, P_c and $\varepsilon_c(H)/\varepsilon_c(0)$ at $T = 2$ K are displayed. Distinct current peaks and valleys in

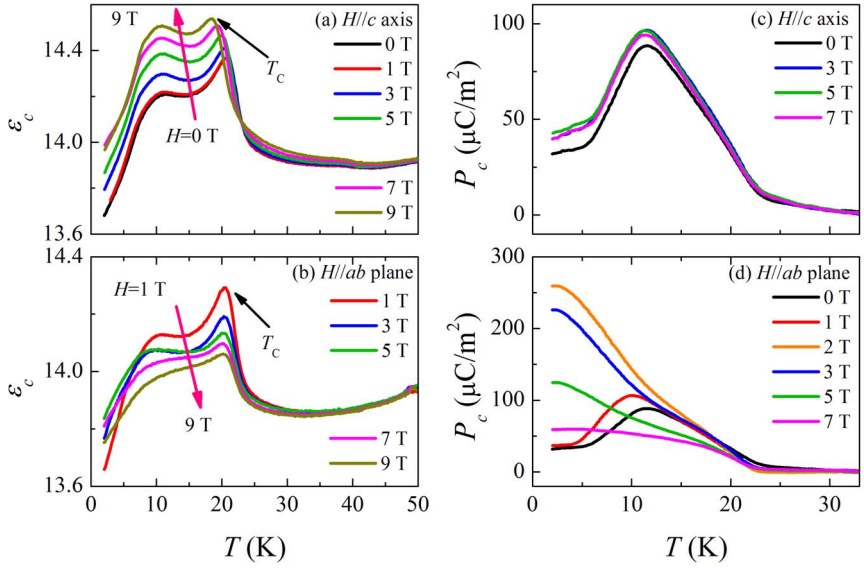

Figure 4 | Measured dielectric susceptibility ε_c in response to H along the c axis (a) and the ab plane (b). Temperature dependence of ferroelectric polarization P_c measured under various magnetic fields: (c) $H//c$ axis, and (d) $H//ab$ plane.

$I(H)$ signal the change (for example flopping or onset) in P_c related to the variation of spin configuration induced by the magnetic field. Accordingly, we can roughly partition the data into three regions, namely, phase I ($H < 1.5$ T), phase II (1.5 T $< H < 4.5$ T), and phase III ($H > 4.5$ T). In phase I, the CM-AFM phase of Dy moment coexists with the SSO phase of Mn, and P_c totally originates from the spirally ordered Mn sublattice, following the DM mechanism. Around $H \sim 1.5$ T, coinciding with the metamagnetic phase transition of Dy in *M(H)* (Fig. 2(b)), the integrated FE polarization P_c (in Fig. 5(b)) exhibits an abrupt increase, which is accompanied by anomaly in $\varepsilon_c(H)$ (in Fig. 5(c)). It suggests the direct effect of the H induced new magnetic orders of Dy on the ferroelectricity, while microscopic evidence is needed to determine whether it is the spiral spin order similar to the case in bulk DMO. In phase II, multicomponent magnetic structures coexist with each other, and P_c reaches a plateau. As $H > 4.5$ T in phase III, P_c is gradually suppressed and hysteresis anomaly can be observed in $\varepsilon_c(H)$, likely indicating the magnetic field induced rotation of the *bc*-spiral (P_c) to the *ab*-spiral (P_a).

A key feature in Fig. 5 is the emergence of the new spin ordering phase of Dy around 1.5 T, which is accompanied by distinct enhancement in P_c. This feature implies dramatic change in the multiferroic domain structure, and thus leading us to expect a different ferroelectric switching behavior along with the phase transition of Dy. Fig. 6(a) shows the *P-E* loops measured under $T = 5$ K and various magnetic fields, in which clear difference in the FE coercive field (E_C) can be observed besides the different polarizations upon increasing *H//ab* plane. In Fig. 6(b), the P_c and E_C is plotted as a function of H. As expected, the P_c shows a sudden increase around $H = 1.5$ T (corresponds to the metamagnetic phase transition of Dy moment), which is well consistent with the pyroelectric current data shown in Fig. 5. Another striking feature is the dramatic increase in E_C around $H = 1.5$ T, which implies a higher energy cost in the ferroelectric switching (or chirality $\boldsymbol{Q}$ switching). A sketch of energy diagram on the FE switching process is plotted in Fig. 6(c). It is clear that the reversal of chirality $\boldsymbol{Q}$ from $\boldsymbol{Q}_a(\boldsymbol{Q}_{-a})$ to $\boldsymbol{Q}_{-a}(\boldsymbol{Q}_a)$ should overcome the barrier coming from the energy difference ΔE between $\boldsymbol{Q}_{a/-a}$ (*bc* spiral) and $\boldsymbol{Q}_{c/-c}$ (*ab* spiral)[43]. Therefore, the larger E_C suggests a higher energy barrier between the *ab* and *bc* spirals (indicated by red dot line in Fig. 6(c)) caused by the emergence of Dy spin order.

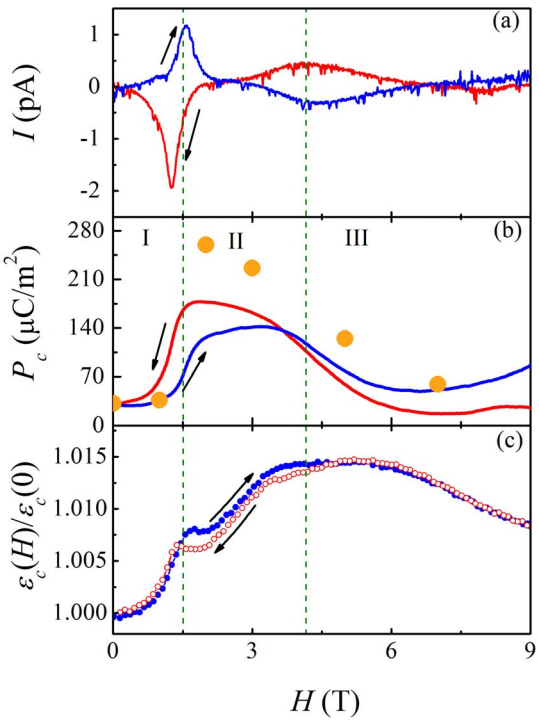

Figure 5 | Isothermal pyroelectric current I_c (a), integrated P_c (b), and ε_c (c) as a function of magnetic field *H//ab* plane measured at $T = 2$ K. The orange dots are the date obtained from the $P_c(T)$ measurements.

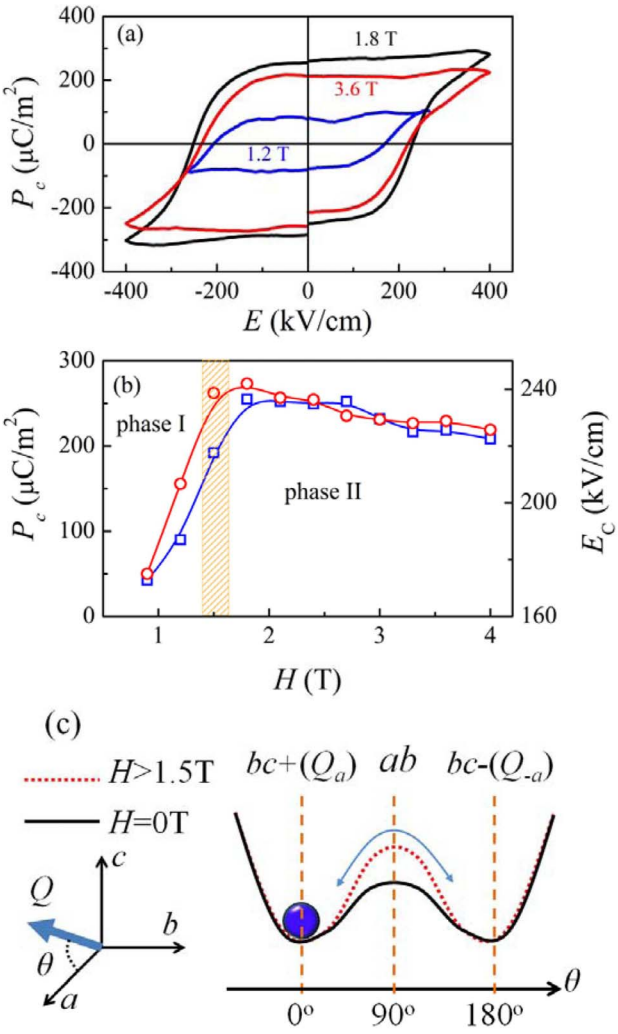

Figure 6 | (a) Ferroelectric hysteresis loops measured under various magnetic field at $T = 5$ K. (b) H dependence of the switching polarization P_c (open squares) and ferroelectric coercive field E_C (open circles) measured using the PUND method. The orange hatched region denotes the magnetic field driven phase transition of Dy moment. (c) A sketch of the energy diagram on the ferroelectric switching process.

Discussion

To this stage, we have demonstrated the magnetic ferroelectricity and ME coupling in DMO thin films. In qualitative sense, the DMO films do show similar physical properties to the bulk counterpart, including the anisotropic magnetism, the SSO phase induced ferroelectricity, and the magnetic field induced polarization enhancement[8,22]. These similarities imply the similar physics of multiferroicity for both thin film and bulk DMO. The present work marks a successful copy of the bulk properties to the thin films for SSO multiferroic rare-earth manganites. In fact, contrast to the case of DMO thin films shown here, so far no ferroelectric polarization has been reported in the TMO thin films[13–18]. A possible reason for this difference is that the DMO locates deeply inside the SSO phase, while the TMO locates in the vicinity of the A-type AFM phase[22]. Therefore, the SSO phase in TMO thin films can be sensitively influenced by perturbations

such as strain, while the SSO phase in DMO thin films shows relatively high stability against the strain.

Even though the substantial similarity in those multiferroic behaviors between the DMO bulk and thin film, one still can identify several quantitative differences in these behaviors between them. First, for DMO thin films, the in-plane and out-of-plane magnetizations are different from those of the bulk as aforementioned, giving rise to a larger magnetic anisotropy $M_m{}^{ab}/M_m{}^{c} \sim 10$ in the thin films. Based on the phase diagram and crystalline structure of perovskite manganites, we note that the a/b ratio exhibits the same trend of evolution with the $GdFeO_3$-type distortion and the Jahn-Teller (JT) effect as the A-site rare-earth element is changed from La to Er, which means the larger a/b value the smaller $GdFeO_3$-type distortion and JT effect[34,44]. Therefore, the larger $a/b \sim 0.916$ in the DMO thin films implies the partial suppression of the JT and $GdFeO_3$-type distortion by the IP compressive strain, as compared with the bulk DMO in which the a/b ratio is 0.905[34]. Consistently, the larger a/b ratio accompanied by the suppression of the JT distortion was also reported for bulk DMO by synchrotron XRD experiments carried out under static pressure[45], which is analogous to the compressive strain in our thin films. Moreover, it is well known that the large JT and $GdFeO_3$-type distortion are responsible for the SSO phase in multiferroic manganites[9–12]. Thus, the compressive strain suppressed JT and $GdFeO_3$-type distortion will weaken the spin-spirals (also the DM interaction) and give rise to a reduced P_c ($\sim$31 $\mu C/m^2$ at 2 K and $H = 0$) in the thin films. From another perspective, according to the model of Mochizuki *et al.*[10–12], which can theoretically reproduce the phase diagram of orthorhombic multiferroic manganites, the DM interaction coexists and competes with the single-ion anisotropy in a way that the *bc*-spiral is favored by the former while the *ab*-spiral is stabilized by the latter. Because of the weakening of DM interaction by strain in the films, more pronounced magnetic anisotropy is thus anticipated, in comparison with the bulk counterpart. Indeed, the magnetism of both bulk and thin film manganites was revealed to well scale with the a/b value[46], which further confirms our explanation on the strain mediated magnetic anisotropy in the DMO thin films.

Besides the magnetic anisotropy, an enhancement in P_c ($P_c(2T)/P_c(0T) \sim 9$ at $T = 2$ K) is observed in the DMO thin films, as shown in Fig. 4(d), which is larger than that ($P_c(2T)/P_c(0T) \sim 3$ at $T = 2$ K) in the bulk counterpart[22]. On one hand, because of the large magnetic anisotropy in the DMO thin films, the possible Dy-spiral phase indeed deserves further microscopic characterization. On the other hand, the above outlined experimental results reveal direct effect of Dy moment on the ferroelectric polarization, which signals the Dy-Mn spin interaction and thus leads us to argue a coherence of spin configurations for Dy and Mn. In fact, the coherence of R and Mn was extensively identified in multiferroic $RMnO_3$ (R = Tb, Dy, Ho) due to the R-Mn spin interaction[31,33,47,48]. Such magnetic structure meets well the configuration of symmetric magnetostriction effect[49–51], that is, each Dy spin chain is sandwiched by two antiferromagnetically coupled Mn spiral spin chains with the same propagation vector. The stacking of the magnetic orders is along the c axis, and the Dy orders would displace cooperatively toward (away) the Mn orders with antiparallel (parallel) spins via the symmetric magnetostriction effect and, as a consequence, polarization along the c axis would be generated, as sketched in Fig. 7(a). Actually, the symmetric magnetostriction effect was proposed as the origin of the polarization enhancement in bulk DMO before the Dy-spiral phase was demonstrated experimentally[52]. Moreover, the symmetric magnetostriction effect between coherent Dy and Mn magnetic orders would also be expected in bulk DMO which has Dy-spiral phase exhibiting the same propagation vector with Mn SSO, as shown in Fig. 7(b). However, the different magnetic anisotropies for thin film and bulk DMO would induce different magnetostriction effects on the polarization, which is the possible origin of the H-induced enhancement in P_c shown in the present work.

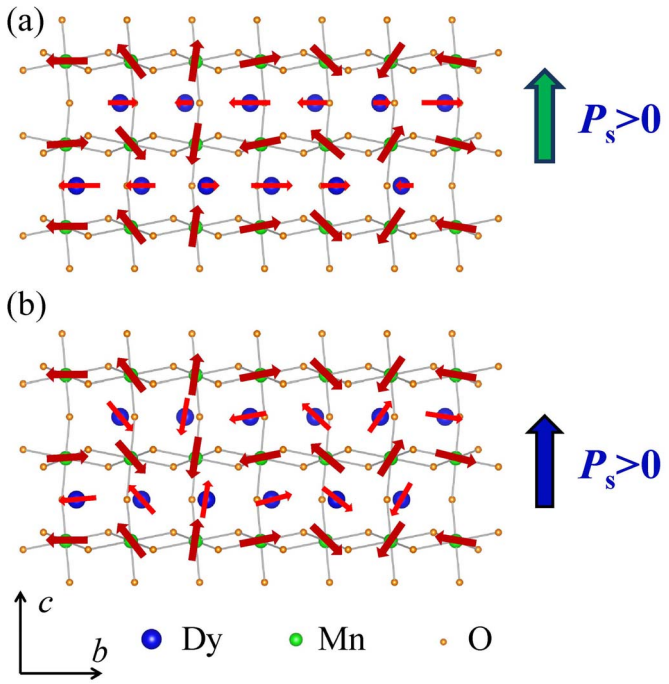

Figure 7 | Sketch of the coherence of magnetic configurations for Dy and Mn spins. (a) the magnetic order of Dy just has the same propagation vector as Mn-spiral phase. (b) Dy has a spiral spin ordering as Mn spins. The both configurations meet the magnetic structure of symmetric magnetostriction effect, and thus possibly leading polarization (P_s) along c axis due to the uniform displacement of Dy.

In summary, multiferroic $DyMnO_3$ thin films are epitaxially grown on Nb-$SrTiO_3$ (001) substrates, and intensively characterized. Our results reveal intriguing multiferroicity in DMO thin film, including i) large magnetic anisotropy $M_m{}^{ab}/M_m{}^{c} \sim 10$ below T_R, which is induced by the compressive strain suppressed $GdFeO_3$-type distortion and Jahn-Teller effect in the thin films; ii) large enhancement in P_c ($\sim$800% at $T = 2$ K) and FE coercive field E_c, which was proposed to be understood by interacting magnetic structures. Our work shows a successful copy of the spiral spin ordering induced multiferroicity from the bulk to thin films, which opens the possibility to integrate such materials into functional devices.

Methods

Pure phase DMO thin films with thickness $t = 300$ nm were epitaxially deposited on (001) Nd-$SrTiO_3$ (NSTO) substrates using pulsed laser deposition (PLD) at 800°C in 0.2 mbar oxygen. KrF excimer laser ($\lambda = 248$ nm) was used with an energy density of $\sim$1 J/cm^2. After the growth, the samples were cooled to room temperature in 400 mbar oxygen ambient at a rate of 5°C/minute. Conducting NSTO substrates were used as both growth templates and bottom electrodes. Detailed crystalline structure investigations, including the normal θ-2θ scan, rocking curve, and the asymmetric reciprocal space mapping, were carried out using a high resolution X-ray diffraction system (Panalytical X-pert Pro). The surface morphology of the film was probed using tapping mode atomic force microscope (Digital Instrument).

Magnetization as a function of T and magnetic field (H) was measured using a Magnetic Properties Measurement System (MPMS, Quantum Design). The cooling and measuring field during the $M(T)$ measurements was fixed at 0.1 T. To obtain the FE polarization along the c axis P_c of the films, square Au top electrodes of 300 μm in diameter were prepared on the film surface, and the pyroelectric current method was used to probe the polarization. For each measurement, the sample was first cooled from 60 to 2 K under a poling electric field of 100 kV/cm. Then, the poling electric field was turned off and the sample was short-circuited for a sufficient period of time to release the charges accumulated on the sample. The pyroelectric current was measured using a Keithley 6514A electrometer during the heating process with a constant ramping rate (2 K/min to 5 K/min). For the pyroelectric current measurements under a magnetic field, H was applied during the poling and the subsequent measuring processes. The ferroelectric hysteresis loops were measured using the positive-up-negative-down (PUND) method (TF Analyzer 2000 from AixACCT Co), and the frequency was set as 100 Hz. The dielectric susceptibility ε_c of the sample with the same device structure was measured using a HP4294A impedance analyzer. The

cryogenic environment and the magnetic field during the pyroelectric current and dielectric susceptibility measurements were provided by a Physical Properties Measurement System (PPMS, Quantum Design).

1. Cheong, S. W. & Mostovoy, M. Multiferroics: a magnetic twist for ferroelectricity. *Nat. Mater.* **6**, 13–20 (2007).
2. Wang, K. F., Liu, J.-M. & Ren, Z. F. Multiferroicity: the coupling between magnetic and polarization orders. *Adv. Phys.* **58**, 321–448 (2009).
3. Ma, J., Hu, J. M., Li, Z. & Nan, C. W. Recent progress in multiferroic magnetoelectric composites: from bulk to thin films. *Adv. Mater.* **23**, 1062–1087 (2011).
4. Tokura, Y. & Seki, S. Multiferroics with spiral spin orders. *Adv. Mater.* **22**, 1554–1565 (2010).
5. Dong, S. N. *et al.* Room temperature multiferroicity in $Bi_{4.2}K_{0.8}Fe_2O_{9+\delta}$. *Sci. Rep.* **3**, 1245 (2013).
6. Zhang, G. H. *et al.* New high T_C multiferroics $KBiFe_2O_5$ with narrow band gap and promising photovoltaic effect. *Sci. Rep.* **3**, 1265 (2013).
7. Kimura, T. *et al.* Magnetic control of ferroelectric polarization. *Nature* **426**, 55–58 (2003).
8. Kimura, T., Lawes, G., Goto, T., Tokura, Y. & Ramirez, A. P. Magnetoelectric phase diagrams of orthorhombic $RMnO_3$ (R = Gd, Tb, and Dy). *Phys. Rev B* **71**, 224425 (2005).
9. Dong, S., Yu, R., Yunoki, S., Liu, J.-M. & Dagotto, E. Origin of multiferroic spiral spin order in the $RMnO_3$ perovskites. *Phys. Rev B* **78**, 155121 (2008).
10. Mochizuki, M. & Furukawa, N. Theory of magnetic switching of ferroelectricity in spiral magnets. *Phys. Rev. Lett.* **105**, 187601 (2010).
11. Mochizuki, M. & Furukawa, N. Microscopic model and phase diagrams of the multiferroic perovskite manganites. *Phys. Rev. B* **80**, 134416 (2009).
12. Mochizuki, M., Furukawa, N. & Nagaosa, N. Spin model of magnetostrictions in multiferroic Mn perovskites. *Phys. Rev. Lett.* **105**, 037205 (2010).
13. Marti, X. *et al.* Emergence of ferromagnetism in antiferromagnetic $TbMnO_3$ by epitaxial strain. *Appl. Phys. Lett.* **96**, 222505 (2010).
14. Kirby, B. J. *et al.* Anomalous ferromagnetism in $TbMnO_3$ thin films. *J. Appl. Phys.* **105**, 07D917 (2009).
15. Cui, Y. M., Tian, Y. F., Shan, A. X., Chen, C. P. & Wang, R. M. Magnetic anisotropy and anomalous transitions in $TbMnO_3$ thin films. *Appl. Phys. Lett.* **101**, 122406 (2012).
16. Tian, Y. F. *et al.* Anomalous exchange bias at collinear/noncollinear spin interface. *Sci. Rep.* **3**, 1094 (2013).
17. Rubi, D. *et al.* Ferromagnetism and increased ionicity in epitaxially grown $TbMnO_3$ films. *Phys. Rev. B* **79**, 014416 (2009).
18. Venkatesan, S., Daumont, C., Kooi, B. J., Noheda, B. & Hosson, J. T. M. D. Nanoscale domain evolution in thin films of multiferroic $TbMnO_3$. *Phys. Rev. B* **80**, 214111 (2009).
19. Han, T. C. & Chao, H. H. Observation of large electric polarization in orthorhombic $TmMnO_3$ thin films. *Appl. Phys. Lett.* **97**, 232902 (2010).
20. Nakamura, M., Tokunaga, Y., Kawasaki, M. & Tokura, Y. Multiferroicity in an orthorhombic $YMnO_3$ single-crystal film. *Appl. Phys. Lett.* **98**, 082902 (2011).
21. Wadati, H. *et al.* Origin of the large polarization in multiferroic $YMnO_3$ thin films revealed by soft- and hard-X-ray diffraction. *Phys. Rev. Lett.* **108**, 047203 (2012).
22. Goto, T., Kimura, T., Lawes, G., Ramirez, A. P. & Tokura, Y. Ferroelectricity and giant magnetocapacitance in perovskite rare-earth manganites. *Phys. Rev. Lett.* **92**, 257201 (2004).
23. Chu, Y.-H., Martin, L. W., Holcomb, M. B. & Ramesh, R. Controlling magnetism with multiferroics. *Mater. Today* **10**, 16–23 (2007).
24. Ratcliff, W. *et al.* Neutron diffraction investigations of magnetism in $BiFeO_3$ epitaxial films. *Adv. Funct. Mater.* **21**, 1567–1574 (2011).
25. Lorenz, B., Wang, Y. Q. & Chu, C-W. Ferroelectricity in perovskite $HoMnO_3$ and $YMnO_3$. *Phys. Rev. B* **76**, 104405 (2007).
26. Fina, I., Fabrega, L., Marti, X., Sanchez, F. & Fonteuberta, J. Chiral domains in cycloidal multiferroic thin films: switching and memory effects. *Phys. Rev. Lett.* **107**, 257601 (2011).
27. Qi, J. *et al.* Coexistence of coupled magnetic phases in epitaxial $TbMnO_3$ films revealed by ultrafast optical spectroscopy. *Appl. Phys. Lett.* **101**, 122904 (2012).
28. Zhang, N., Dong, S. & Liu, J.-M. Ferroelectricity generated by spin-orbit and spin-lattice coupling in multiferroic $DyMnO_3$. *Front. Phys.* **7**, 408–417 (2012).
29. Zhang, N. *et al.* Ho substitution suppresses collinear Dy spin order and enhances polarization in $DyMnO_3$. *Appl. Phys. Lett.* **99**, 102509 (2011).
30. Schierle, E. *et al.* Cycloidal order of 4*f* moments as a probe of chiral domains in $DyMnO_3$. *Phys. Rev Lett.* **105**, 167207 (2010).
31. Feyerherm, R. *et al.* Magnetic-field induced effects on the electric polarization in $RMnO_3$(R = Dy,Gd). *Phys. Rev. B* **79**, 134426 (2009).
32. Feyerherm, R., Dudzik, E., Aliouane, N. & Argyriou, D. N. Commensurate Dy magnetic ordering associated with incommensurate lattice distortion in multiferroic $DyMnO_3$. *Phys. Rev. B* **73**, 180401(R) (2006).
33. Prokhnenko, O. *et al.* Enhanced ferroelectric polarization by induced Dy spin order in multiferroic $DyMnO_3$. *Phys. Rev Lett.* **98**, 057206 (2007).
34. Alonso, J. A., Lope, M. J. M., Casais, M. T. & Díaz, M. T. F. Evolution of the Jahn−Teller distortion of MnO6 octahedra in RMnO3 perovskites (R = Pr, Nd, Dy, Tb, Ho, Er, Y): A neutron diffraction study. *Inorg. Chem.* **39**, 917–923 (2000).
35. Daumont, C. J. M. *et al.* Epitaxial $TbMnO_3$ thin films on $SrTiO_3$ substrates: a structural study. *J. Phys.: Condens. Matter.* **21**, 182001 (2009).
36. Midya, A., Das, S. N., Mandal, P., Pandya, S. & Ganesan, V. Anisotropic magnetic properties and giant magnetocaloric effect in antiferromagnetic $RMnO_3$ crystals (R = Dy, Tb, Ho, and Yb). *Phys. Rev B* **84**, 235127 (2011).
37. Aharoni, A. Demagnetization factors for rectangular ferromagnetic prisms. *J. Appl. Phys.* **83**, 3432–3434 (1998).
38. Harikrishnan, S. *et al.* Phase transitions and rare-earth magnetism in hexagonal and orthorhombic $DyMnO_3$ single crystals. *J. Phys.: Condens. Matter* **21**, 096002 (2009).
39. Okuyama, D. *et al.* Magnetically driven ferroelectric atomic displacements in orthorhombic $YMnO_3$. *Phys. Rev B* **84**, 054440 (2011).
40. Picozzi, S., Yamauchi, K., Sanyal, B., Sergienko, I. A. & Dagotto, E. Dual nature of improper ferroelectricity in a magnetoelectric multiferroic. *Phys. Rev. Lett.* **99**, 227201 (2007).
41. Hou, Y. S., Yang, J. H., Gong, X. G. & Xiang, H. J. Prediction of a multiferroic state with large electric polarization in tensile strained $TbMnO_3$. *Phys. Rev. B* **88**, 060406(R) (2013).
42. Yamasaki, Y. *et al.* Electric control of spin helicity in a magnetic ferroelectric. *Phys. Rev. Lett.* **98**, 147204 (2007).
43. Mochizuki, M. & Nagaosa, N. Theoretically predicted picosecond optical switching of spin chirality in multiferroics. *Phys. Rev. Lett.* **105**, 147202 (2010).
44. Kimura, T. *et al.* Distorted perovskite with e_g^1 configuration as a frustrated spin system. *Phys. Rev B* **68**, 060403(R) (2003).
45. Chen, J. M. *et al.* Pressure-dependent electronic structures in multiferroic $DyMnO_3$: A combined lifetime-broadening-suppressed x-ray absorption spectroscopy and *ab initio* electronic structure study. *J. Chem. Phys.* **133**, 154510 (2010).
46. Fontcuberta, J. *et al.* Ferroelectricity and strain effects in orthorhombic YMnO3 thin films. *Phase Transitions* **84**, 555–568 (2011).
47. Prokhnenko, O. *et al.* Coupling of frustrated Ising spins to the magnetic cycloid in multiferroic $TbMnO_3$. *Phys. Rev. Lett.* **99**, 177206 (2007).
48. Brinks, H. W. *et al.* Crystal and magnetic structure of orthorhombic $HoMnO_3$. *Phys. Rev B* **63**, 094411 (2001).
49. Lee, N. *et al.* Mechanism of exchange striction of ferroelectricity in multiferroic orthorhombic $HoMnO_3$ single crystals. *Phys. Rev. B* **84**, 020101(R) (2011).
50. Tokunaga, Y., Iguchi, S., Arima, T. & Tokura, Y. Magnetic-field-induced ferroelectric state in $DyFeO_3$. *Phys. Rev. Lett.* **101**, 097205 (2008).
51. Stroppa, A., Marsman, M., Kresse, G. & Picozzi, S. The multiferroic phase of $DyFeO_3$: an ab initio study. *New J. Phys.* **12**, 093026 (2010).
52. Feyerherm, R., Dudzik, E., Prokhnenko, O. & Argyriou, D. N. Rare earth magnetism and ferroelectricity in $RMnO_3$. *J. Phys.: Conf. Ser.* **200**, 012032 (2010).

Acknowledgments

This work was supported by the National Natural Science Foundation of China (Grant Nos. 11104090, 11374112, 11234005, 51332006, 11004027), the National 973 Projects of China (Grant No. 2011CB922101). The XRD-RSM and PUND were performed at Max-Planck Institute of Microstructure Physics, Halle, Germany. Thanks are due to Prof. Dietrich Hesse, Dr. Marin Alexe, and Dr. Ignasi Fina for this possibility, and for fruitful discussions.

Author contributions

C.L.L., T.W. and J.M.L. conceived and designed the experiments. C.L.L. and Z.B.Y. carried out the experiments. C.L.L., S.D., T.W. and J.M.L. wrote the paper. Z.C.X., H.L., H.W.W., Z.M.T. and S.L.Y. reviewed and commented on the paper. All the authors discussed the results and commented on the manuscript.

Additional information

Competing financial interests: The authors declare no competing financial interests.

How to cite this article: Lu, C. *et al.* Polarization enhancement and ferroelectric switching enabled by interacting magnetic structures in $DyMnO_3$ thin films. *Sci. Rep.* **3**, 3374; DOI:10.1038/srep03374 (2013).